A smart device for particle separation in water using ultrasonic standing waves

Y.S. Lee and J.H. Kwon

Smart Measurement Group, Korea Research Institute of Standards and Science, Doryong-Dong No.1, Daejeon, South Korea (E-mail: *yslee@kriss.re.kr*; *jhkwon@kriss.re.kr*)

Abstract This paper presents the theory, design, and evaluation of a smart device for the enhanced separation of particles mixed in fluid. The smart device takes advantage of the ultrasonic standing wave, which was generated by the operation of a piezoceramic PZT patch installed in the smart device. The details of the device design including the electro-acoustical modelling for separation and PZT transducer are described. Based on this design, the separation device was fabricated and evaluated. In the experiments, an optical camera with a zoom lens was used to monitor the position of interested particles within the separation channel layer in the device. The electric impedance of the PZT patch bonded on the separation device was measured. The device shows a strong levitation and separation force against 50 μm diameter particles mixed with water at the separation channel in the device. Experimental results also showed that the device can work with both heavy and light sand particles mixed with water due to the generated standing wave field in the separation channel.

Keywords Acoustic impedance; acoustic pressure; electro-acoustic; particle separation; piezoelectric actuator; ultrasonic standing wave

Water Science and Technology: Water Supply **Vol 6 No 1 pp 173–183**

Introduction

Ultrasonic standing waves have been widely used in various fields including environmental technology, cell handling in biotechnology, microfluidics and so on (Hawkes and Coakley, 2001; Hill *et al.*, 2002). Since it has been known that standing waves at high frequency can separate, concentrate and mix particles with relevant fluids in a given channel, the research area is rapidly getting broader and broader.

The technology of an ultrasonic standing wave device is very much related to piezoelectric transducers and fluid flow, especially when the device is designed with micro electro-mechanical systems (MEMS). Hill *et al.* (2002) showed the importance of the modelling of the piezoelectric transducers and the wave propagation in a multi-layered device in order to generate an exact standing wave field in a separation channel.

On this basis in this paper, a theoretical consideration and modelling of an ultrasonic separation device are described in the methods section, which contains the concept and electro-acoustical modelling. Especially, the modelling of the piezoceramic transducer in terms of the acoustic impedance and transfer matrix is analyzed in detail. In the design and analysis section, the design of the separation device is discussed with actual operation methodology and initial measurement. The experimental set-up and results are discussed in the results and discussion section with relevant data and observed phenomena.

Methods

Concept of separation with standing wave

The concept of the separation device in this study can be illustrated as shown in Figure 1. The cavity channel in the separation device is designed to generate an acoustic pressure

doi: 10.2166/ws.2006.022

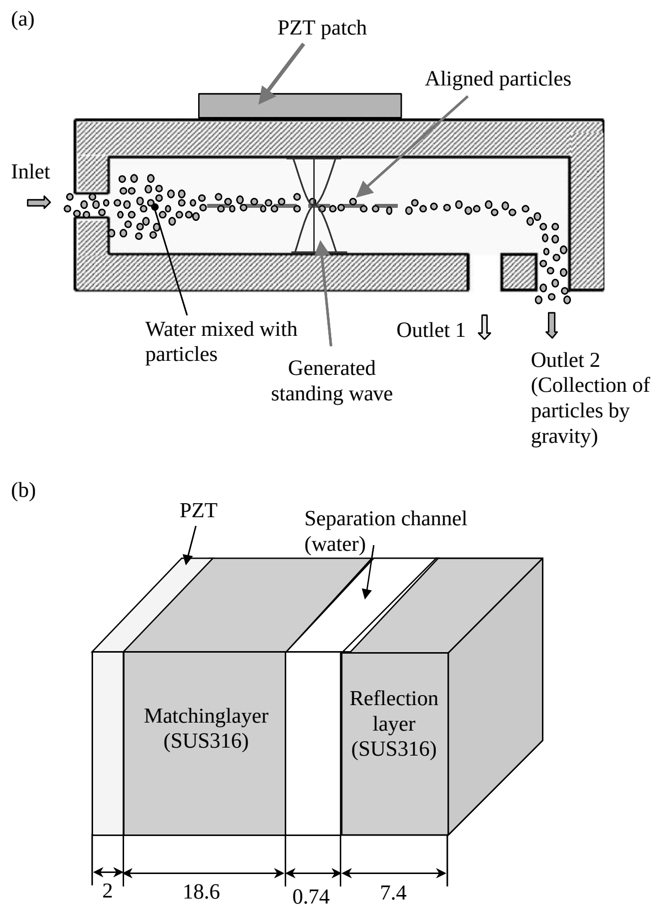

Figure 1 A smart separation device with ultrasonic standing wave: (a) concept; (b) separator design

field with a standing wave. A half-wavelength of acoustic wave in the channel makes a nodal line of zero acoustic pressure at the middle of the channel. The acoustic wave is primarily activated by a piezoceramic PZT (piezoelectric zirconate titanate) patch which is bonded on the top of the device (Desilets *et al.*, 1978).

The separation device for ultrasonic standing wave formation consists of a PZT patch, matching layer of SUS316, separation channel and reflection channel of SUS316 as can be seen from Figure 1(b). The PZT patch of Fuji Ceramics C-7 was length × width × thickness = 20 × 5 × 2 mm, which resonates at about 1.0 MHz for its first thickness vibration mode. The PZT patch was bonded on the matching layer, which transfers the PZT vibration to the separation channel. The thickness of the matching layer was designed to be 18.6 mm, which is exactly three times the unit wavelength of 6.2 mm at 1.0 MHz in SUS316.

In SUS316, the wave speed is assumed as 6,200 m/sec. The separation channel is 0.74 mm long, which is exactly the same as the half wavelength at 1.0 MHz in water and in this case the wave speed was assumed as 1,480 m/sec. Also the nodal line of the ultrasonic pressure field was designed to be located at the middle of the separation channel height as shown in Figure 1. The reflection layer is 7.4 mm to meet one and a quarter times the unit wavelength at the same frequency in SUS316.

Separation condition

In this particle separation using the acoustic standing wave field, the separability of particles in fluid depends upon the pressure gradient in the separation channel. As illustrated in Figure 2, the pressure gradient defined by $\theta = 2P_{\max}/h$, where $P_{\max}$ and h are the maximum pressure magnitude and the height at the separation channel with 1/2 wavelength. If it is assumed that a particle to be separated in fluid is a solid sphere of diameter d, the particle experiences three different forces: gravitational force W, buoyancy B and acoustic force F_A. The resultant force applied to a particle above the pressure nodal line is $F_A + W - B$, but one below the nodal line is $F_A + B - W$. Hence the acoustic force must satisfy the following condition to separate particles in fluid as

$$F_A > |W - B| \tag{1}$$

The acoustic force F_A applied to a particle can then be calculated with

$$F_A = \Delta p \cdot S \tag{2}$$

where $\Delta p = \theta \cdot d_e$ is the acoustic pressure difference between the top and bottom half-spheres of the particle, which is assumed to always be positive, $d_e \approx d/3$ is the effective distance between the acoustic pressure centres of each half-sphere, and S is the sectional area of the sphere particle. Therefore, the maximum pressure required to separate the solid particle could be given as

$$P_{\max} > \frac{6h}{\pi d^3} \cdot |W - B| \tag{3}$$

Equation (3) represents the necessary condition to separate certain particles with the acoustic standing wave. Thus the acoustic pressure gradient decides the controllable particle mass.

Electro-acoustical modelling

The schematic diagram for electro-acoustical modelling of an ultrasonic separator is shown in Figure 3. It consists of a PZT plate, air backing, matching layer (SUS316), separation channel layer (water), reflection layer (SUS316) and another air backing.

If Z_f and Z_b denote the front and back load impedance of the piezoceramic PZT patch respectively, the acoustic impedance from the PZT to the backing Z_{ib} and the acoustic

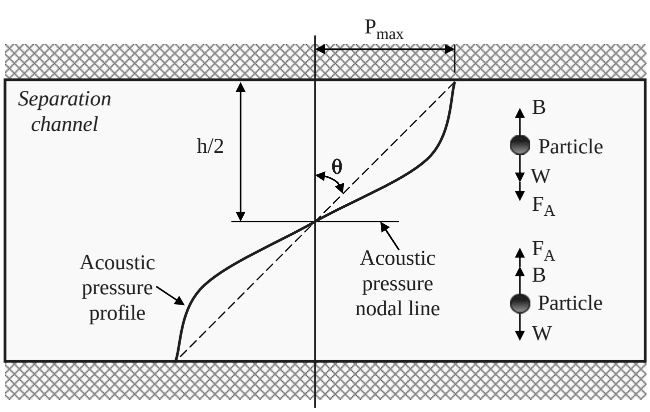

Figure 2 Pressure gradient and exerting forces at particles in acoustic separation device

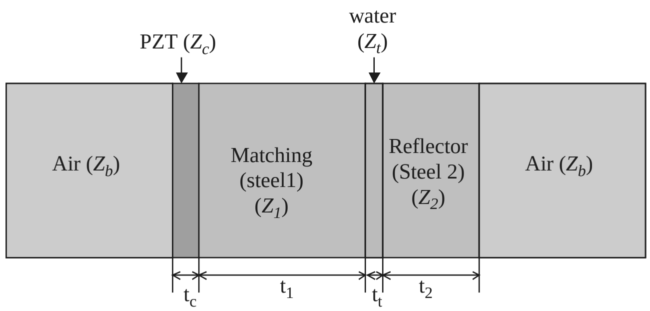

Figure 3 Schematic diagram of ultrasonic separator for electro-acoustical analysis

impedance from the PZT to the front matching layer Z_{if} are given by (Kinsler *et al.*, 1982)

$$Z_{ib} = Z_c + \frac{Z_b + jZ_c \tan\theta_c}{Z_c + jZ_b \tan\theta_c} \qquad Z_{if} = Z_c \frac{Z_f + jZ_c \tan\theta_c}{Z_c + jZ_f \tan\theta_c} \tag{4}$$

The acoustic input impedance in the centre of the PZT patch Z_{in} is the summation of Z_{ib} and Z_{if} in parallel; therefore Z_{in} is given by

$$Z_{in} = \frac{Z_{ib}Z_{if}}{Z_{ib} + Z_{if}} \tag{5}$$

The impedance to the front matching layer at piezoceramic plate, Z_f in Equation (4), is written with

$$Z_f = Z_1 \frac{Z_{tf} + jZ_1 \tan\theta_1}{Z_1 + jZ_{tf} \tan\theta_1} \tag{6}$$

where Z_{tf} is the impedance to the front separation channel layer at the boundary between the matching layer and the separation channel layer, which is given by

$$Z_{tf} = Z_t + \frac{Z_{2f} + jZ_t \tan\theta_t}{Z_t + jZ_{2f} \tan\theta_t} \tag{7}$$

where Z_{2f} is the impedance to the front reflection layer at the boundary of the separation channel layer and the reflection layer, which is expressed by

$$Z_{2f} = Z_2 + \frac{Z_b + jZ_2 \tan\theta_2}{Z_2 + jZ_b \tan\theta_2} \tag{8}$$

where $\theta_i = t_i\omega/v_i$.

Design and analysis

Design of separation device. In order to demonstrate the separation of wet sand particles from mixed water, a smart separation device has been manufactured based on the description in the previous section. The particle separation device has been designed as plotted in Figure 4(a), which is 115 mm long, 26.74 mm high except the PZT patch and 7 mm wide. The device is made of SUS316 and has a separation channel 97 mm long, and one inlet and two outlets. One of the outlets is for the collection of sand particles and the other is for clean water. The cross-sectional area of each outlet is 1.5 × 0.74 mm and is exactly half of the inlet's (3.0 × 0.74 mm), which allows the continuity of fluid flow in the separation channel.

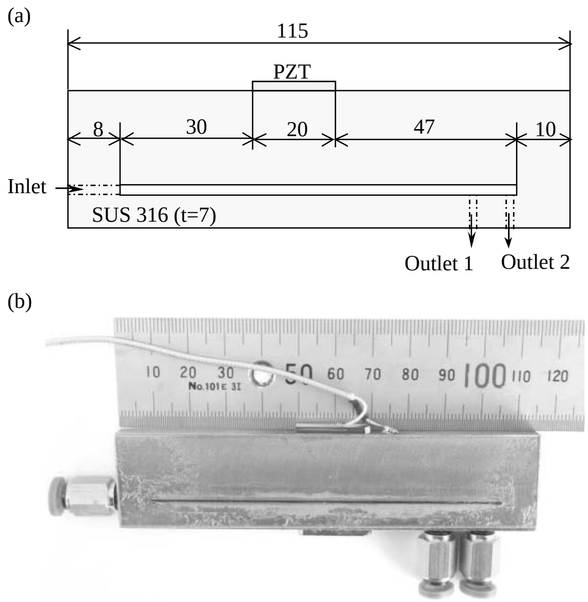

Figure 4 The separation device: (a) design and dimension; (b) photograph

The PZT patch was bonded on the top side of the device and is positioned 30 mm away from the end of the inlet hole in the separation channel as shown in Figure 4(a). The fluid flow inside the separation channel could be turbulent after passing through the inlet hole and the turbulent flow could be sustained up to a certain distance. As the ultrasonic separator requires laminar flow at its standing wave field in the channel to be operated properly, the distance of 30 mm allows the turbulent flow to change into laminar flow. As can be seen from Figure 4(b), the device is made as one body which is much simpler than other previous ultrasonic separators. A pair of acrylic plates is bonded on either side of the separation device which gives a transparent view from the outside to the inside of the channel.

Finite element analysis. A finite element model has been created to estimate the acoustic pressure response inside the separation channel in terms of time. As shown in Figure 4(a), the designed model is drawn schematically to present the structure of the separator. The rectangle with dashed lines in Figure 5(a) is the finite element modelled part. Figure 5(b) is the 2-dimensional finite element model, which includes the PZT plate, matching and reflection layers and separation filled with fresh water. The separation channel with water has been modelled with seven points (p1–p7) to show acoustic variation.

The finite element analysis shows that the acoustic standing wave in the channel can be constructed within a very short time after the excitation of the PZT patch. As shown in Figure 6(a), it takes about 5 μsec to form a minute standing wave field and more than 10 μsec makes the field five times stronger, and another 10 μsec develops it 10 times stronger. The acoustic pressure nodal point of 1/2 wavelength is constructed at p4 of the channel as plotted in Figure 6(b), where particles in water can be gathered. If the thickness of each layer in the separation device is not carefully chosen, the effective standing wave field cannot be generated.

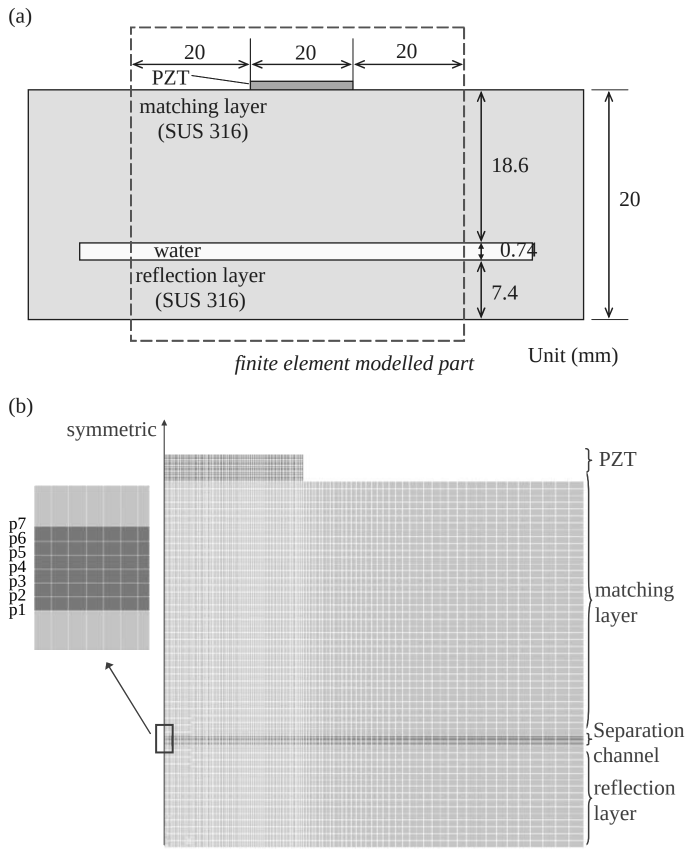

Figure 5 Finite element model: (a) modelled part; (b) modelling (1/2 with symmetry)

Figure 7 shows the acoustical pressure field in the separation channel, where the standing wave is constructed with the positive pressure at the upper part and negative pressure at the lower part. Although the largest pressure magnitude is built just below the PZT patch part, the pressure field stretches effectively 1/2 length of the PZT patch to both ends. It is thus demonstrated by Figure 7 that the particles in fluid will begin to separate at 1/2 length of the PZT patch before the left end of the PZT patch, and they will mix again at the symmetric point. Thus the separation zone could be twice the PZT length. The length of separation zone can be enlarged by the increase of the applied voltage to the PZT patch.

Measured impedance. Electrical impedance of the PZT patch bonded to the separation device has been measured before the separation experiment with a Hewlett-Packard 4194A Impedance Analyzer in the frequency range of 0.5–1.5 MHz as shown in Figure 8. The impedance was measured both when the separation channel is empty (with air) and full with water. As the frequency designed to make standing wave is 1.0 MHz, a clear resonance has been observed at the frequency as plotted in Figure 6. It is noted that the impedance with water is a little bit different from that with air. This is because the water in the channel has a larger impedance than air.

Results and discussion

As shown in Figure 9, the ultrasonic smart separation device was installed with fittings on a flat test bed. The device was clamped partly by a mechanical vice to hold it

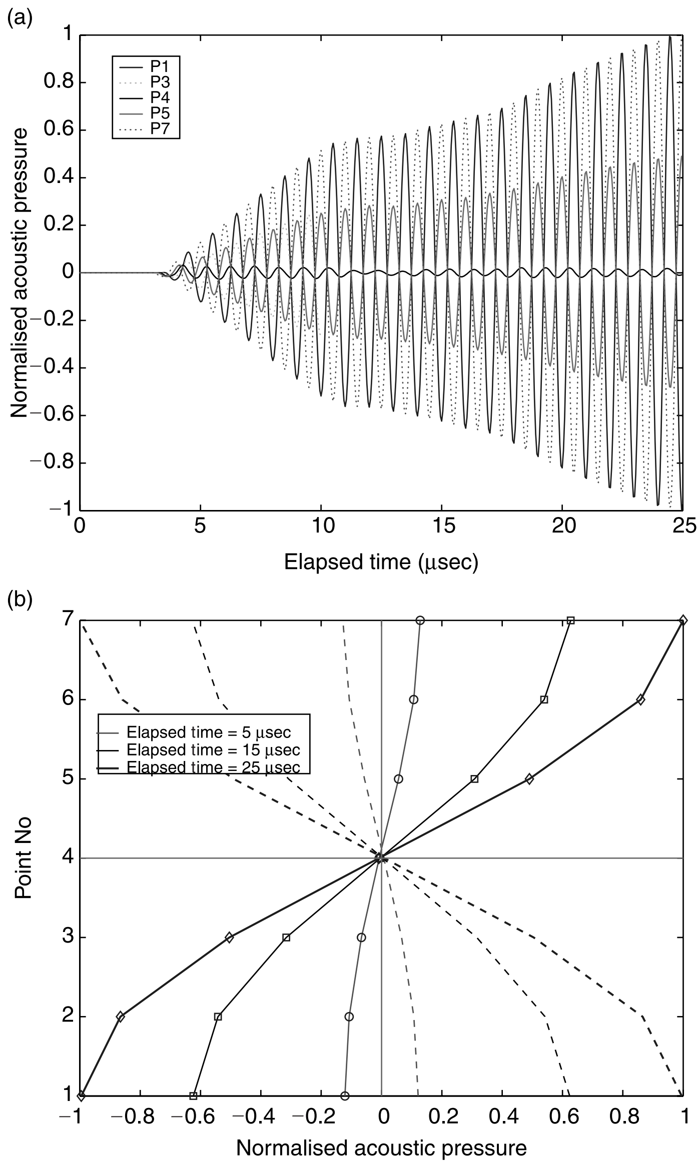

Figure 6 Finite element analysis results: (a) pressure field vs elapsed time; (b) standing wave formation with time

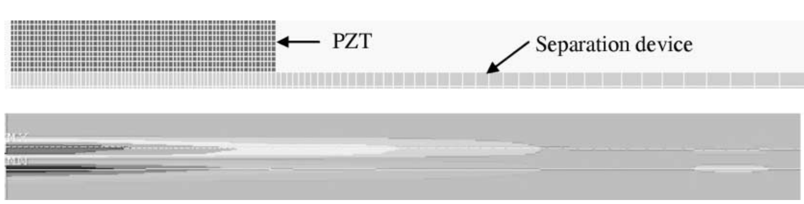

Figure 7 Construction of acoustic pressure field in the separation channel (1/2 with symmetry)

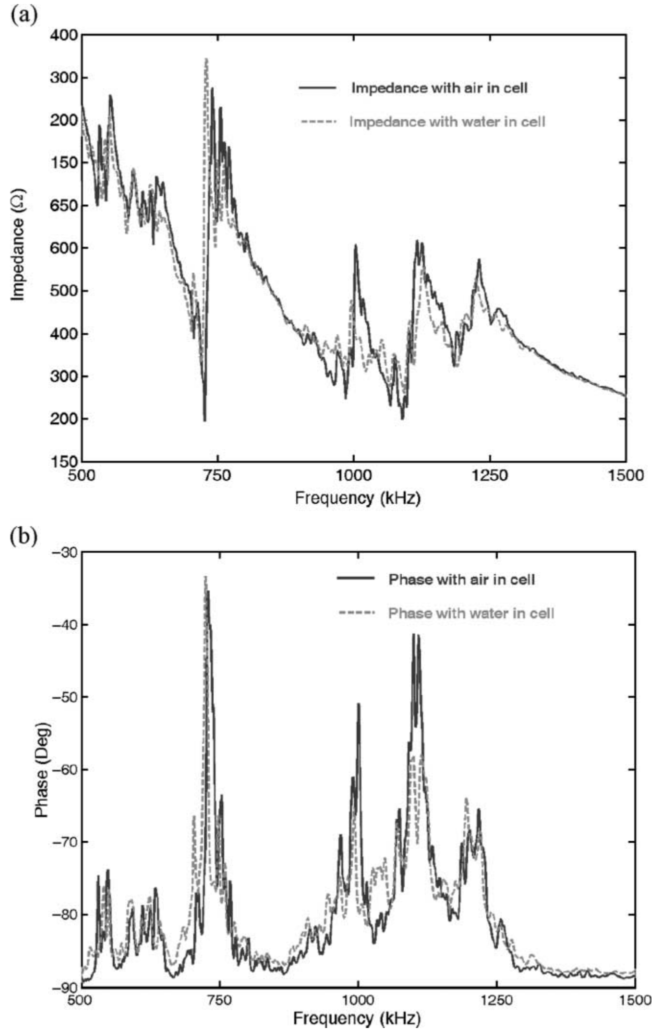

Figure 8 Measured impedance of the PZT patch bonded on the smart separation device

firmly, and inlet and outlet tubes with the inner diameter of 2.5 mm were connected to and from it. The power amplifier used in the experiment is the T&C Power Conversion Inc. AG Series Ultrasonic Amplifier for the actuation of the PZT patch with 1.0 MHz. The power signal to the PZT has been monitored with a LeCroy 9354A oscilloscope.

The particles for separation in the experiment were sand which is about 50 microns in diameter. The particles were mixed with water and were delivered to the separation device by gravity. The inlet tube was connected to two different separate funnels with valves as shown in Figure 4: one is for water and the other is for sand particles. The valves were used to control the flow speed of the mixed water. A CCD camera with an optical zoom lens was installed to observe and record the separation during the experiment.

A levitation test of sand particles has been made in order to observe the formation of 1.0 MHz ultrasonic standing wave in the separation channel at the device. After the sand mixed water had filled the separation channel, all of the inlet and outlet valves were closed. The levitation test was begun after the sand particles had settled on the bottom of the channel as shown in Figure 10(a). As shown in Figure 10(b), the particles were

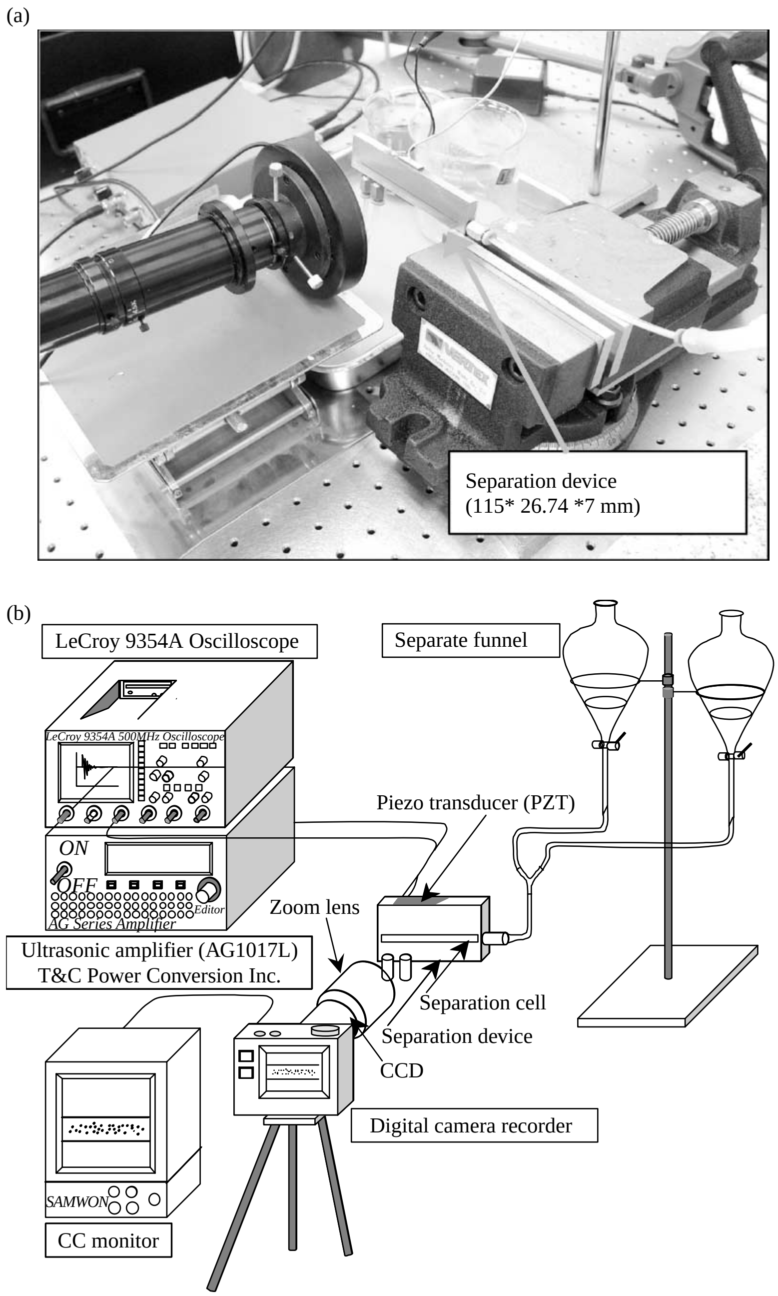

Figure 9 Experimental set-up with the smart separation device: (a) photograph; (b) separation test arrangement

arranged in a line at the nodal line of the standing wave when the PZT was oscillated at its thickness mode with ± 50 V. Because the particles used in the experiment were more or less sticky, the particles in photographs of Figure 10 were aggregated to each other as a cloud.

Also the particles in Figure 10 are relatively heavy and it is shown that they are a little bit low located from the nodal line (the middle of the separation channel) of the generated standing wave field. The movement of the cloud of the particles from the

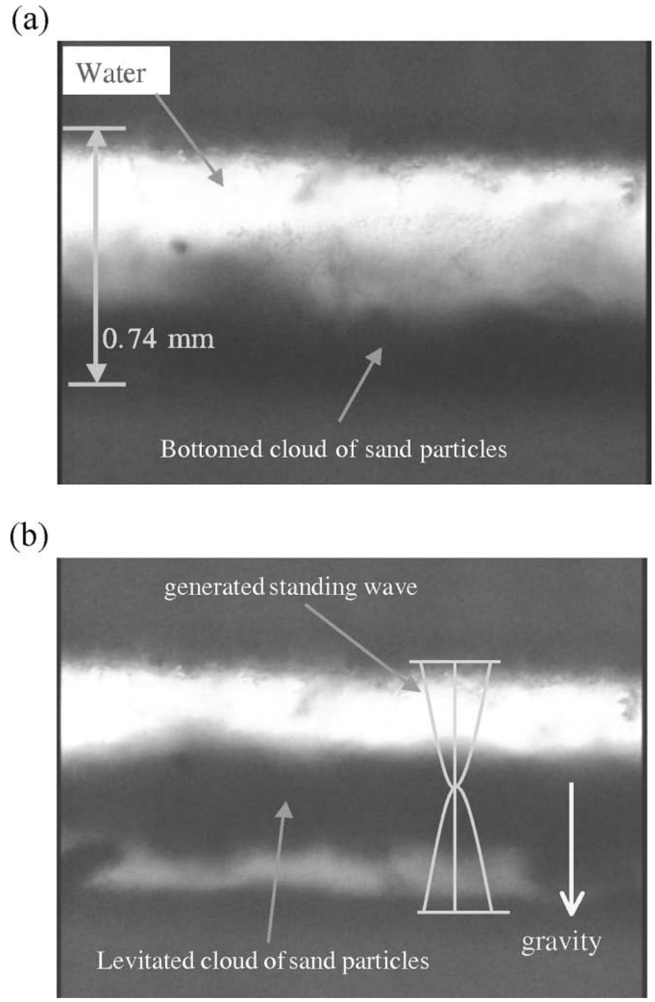

Figure 10 Levitation of heavy sand particles cloud using ultrasonic standing wave: (a) before; (b) after

bottom to the nodal line was very quick at the given frequency of 1.0 MHz when the electric power was applied to the PZT actuator. The experiment with light particles is shown in Figure 11, which can be compared with Figure 10.

It is noted that the continuous levitation and drop of the particle clouds by on and off of the power amplifier with the change of frequency in a limit range, say $\pm 10-20$ kHz, made the cloud shift in parallel, rotate and mix.

Conclusions

In this study, the design, modelling and experiment of a smart separation device using an ultrasonic standing wave device has been described. The device design, including the electro-acoustical modelling for separation and PZT transducer, is investigated and discussed. In the experiments, the electric impedance of the PZT patch bonded on the separation device was measured at first, which showed a clear resonance at the designed frequency of 1.0 MHz. Experimental results showed that the device can levitate settled sand particles on the bottom to the nodal line of the standing wave field of the separation channel.

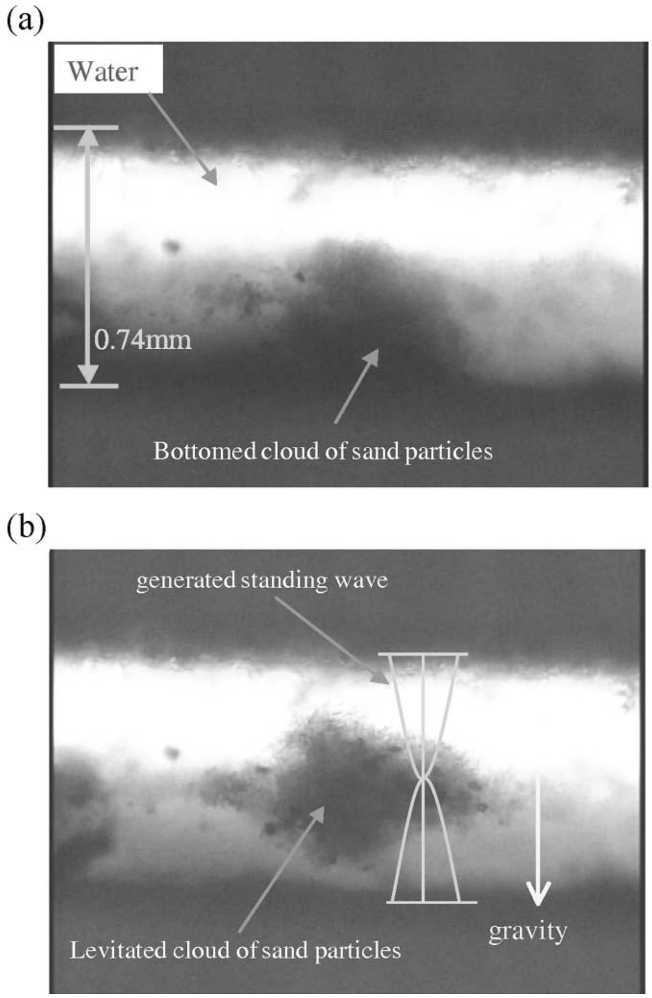

Figure 11 Levitation of light sand particles cloud using ultrasonic standing wave: (a) before; (b) after

References

Desilets, C.S., Fraser, J.D. and Kino, G.S. (1978). The design of efficient broad-band piezoelectric transducers. *IEEE Transactions on Sonics and Ultrasonics*, **25**(3), 115–125.

Hawkes, J.J. and Coakley, W.T. (2001). Force field particle filter, combining ultrasound standing waves and laminar flow. *Sensors and Actuators B*, **75**, 213–222.

Hill, M., Shen, Y. and Hawkes, J.J. (2002). Modelling of layered resonators for ultrasonic separation. *Ultrasonics*, **40**, 385–392.

Kinsler, L.E., Frey, A.R., Coppens, A.B. and Sanders, J.V. (1982). *Fundamentals of Acoustics* (3rd edn), Wiley, New York.